# Mathematical Modeling as a Tool to Investigate the Design and Operation of the Zymotis Packed-Bed Bioreactor for Solid-State Fermentation

**D. A. Mitchell,* O. F. von Meien**

*Departamento de Engenharia Química, Universidade Federal do Paraná, Cx. P. 19011, 81531-970 Curitiba, Paraná, Brazil; e-mail: davimitc@engquim.ufpr.br*

*Received 25 February 1999; accepted 17 September 1999*

**Abstract:** Zymotis bioreactors for solid-state fermentation (SSF) are packed-bed bioreactors with internal cooling plates. This design has potential to overcome the problem of heat removal, which is one of the main challenges in SSF. In ordinary packed-bed bioreactors, which lack internal plates, large axial temperature gradients arise, leading to poor microbial growth in the end of the bed near the air outlet. The Zymotis design is suitable for SSF processes in which the substrate bed must be maintained static, but little is known about how to design and operate Zymotis bioreactors. We use a two-dimensional heat transfer model, describing the growth of *Aspergillus niger* on a starchy substrate, to provide guidelines for the optimum design and operation of Zymotis bioreactors. As for ordinary packed-beds, the superficial velocity of the process air is a key variable. However, the Zymotis design introduces other important variables, namely, the spacing between the internal cooling plates and the temperature of the cooling water. High productivities can be achieved at large scale, but only if small spacings between the cooling plates are used, and if the cooling water temperature is varied during the fermentation in response to bed temperatures.  *Biotechnol Bioeng* **68**: 127–135, 2000.
**Keywords:** solid-state fermentation; bioreactor design; bioreactor operation; mathematical modeling; packed-bed bioreactors

## INTRODUCTION

Solid-state fermentation (SSF) involves the growth of microorganisms on moist solid substrates in the absence of visible water between the substrate particles. SSF has advantages over submerged liquid fermentation for the production of certain microbial products. One important example is fungal spore production: many fungi do not sporulate well in liquid culture (Boyette et al., 1991) and, in any case, in the production of fungal spores for use as biopesticides, spores produced in submerged liquid fermentation are more sensitive, less stable, and less virulent than the aerial spores produced in the environment provided by SSF (Morin, 1992).

For some SSF processes the substrate bed must remain static throughout the growth phase. The bed must remain static in fungal spore production because agitation can damage the reproductive hyphae, greatly reducing spore yields (Silman, 1980). Static beds are also required when the substrate particles are required to be knitted together by the fungal mycelium, such as in the production of fermented foods like tempe.

Two bioreactor designs are available for static SSF processes, the tray and the packed-bed. The packed-bed has advantages over the tray because the forced aeration allows better control of environmental conditions in the bed, due to the ability to manipulate the temperature and flowrate of the process air (Sangsurasak and Mitchell, 1995). However, in ordinary packed beds, which lack internal heat transfer plates, an axial temperature gradient is established within the bed. Temperatures over 20°C above the inlet air temperature can be reached in the upper regions of the bed (Ghildyal et al., 1994), restricting growth and product formation. This limits the height of the bed which can be used (Sangsurasak and Mitchell, 1995). Axial temperature gradients can be reduced by promoting radial heat transfer. Saucedo-Castaneda et al. (1990) used a 6-cm diameter packed bed bioreactor with cooling of the external surface. Radial heat transfer dominated, and as a result of the reduced axial temperature gradient, theoretically, a tall bioreactor could be used. However, for a large-scale process it is impractical to use cylindrical beds of only 6-cm diameter, because the beds would have to be very tall to hold large amounts of substrate.

The solution provided by Roussos et al. (1993), with the Zymotis bioreactor, was to use a wide packed bed, but to insert vertical heat transfer plates into the bed to promote horizontal heat transfer by conduction. The work done by Roussos et al. (1993) was experimental, and did not systematically appraise the effect of design and operating conditions on bioreactor performance. The aim of the present work is to use modeling to provide guidelines for the design and operation of a Zymotis bioreactor.

* *Present address:* Department de Solos, Universidade Federal do Paraná, Rua dos Funcionàrios 1540, Juvevê, Curitiba 80035-050, Paraná, Brazil; e-mail: mitchell@agrarias.ufpr.br
*Correspondence to:* D.A. Mitchell

## MODEL DEVELOPMENT

### System and Assumptions

The Zymotis bioreactor of Roussos et al. (1993) is a rectangular packed-bed bioreactor, aerated from the bottom with moist air (Fig. 1). During the process the substrate bed remains static. The outer casing is assumed to be made of an insulating material, such that there are no temperature gradients from front to back in the bioreactor. The system modeled is a repeating unit within this bioreactor (Fig. 2). The model concentrates on the heat transfer phenomena. Equations for mass transfer have not been incorporated. Sangsurasak and Mitchell (1998) discussed most of the assumptions in the current model, in the context of heat transfer in an ordinary packed bed. Since their model described well the experimental data of Saucedo-Castaneda et al. (1990) and Ghildyal et al. (1994), the assumptions are accepted as reasonable.

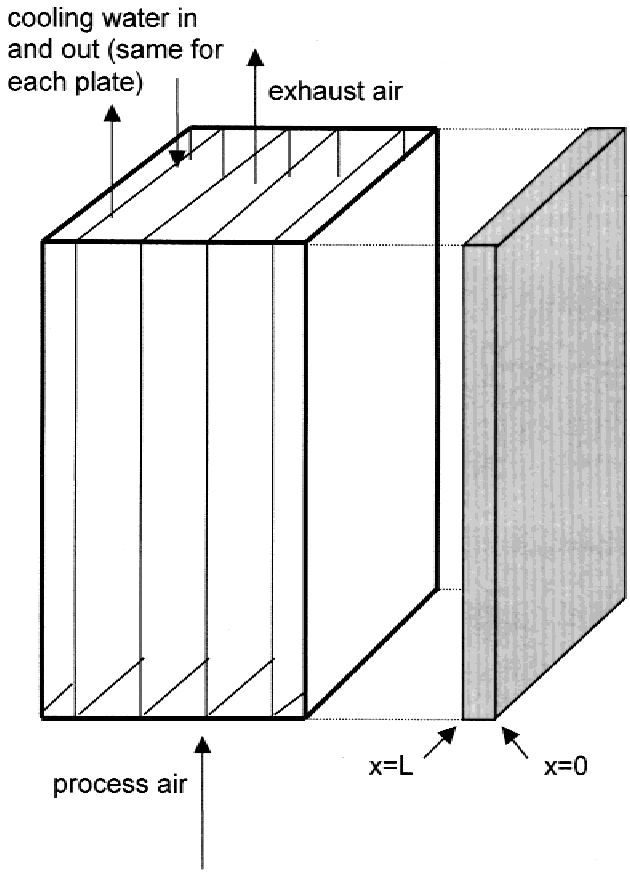


**Figure 1.** Diagram of the Zymotis reactor, which consists of an outer casing (indicated with the thicker lines and made transparent to show internal detail), and internal vertical rectangular cooling plates (four of which are shown). Substrate is loaded into the spaces between the cooling plates. The bioreactor can be considered to contain a number of identical substrate slabs, each of which extends from a plate surface to the mid-point between two adjacent plates. There is no heat transfer across the plane midway between the plates (i.e., at $\times = 0$). The slabs at the right and left hand ends are made identical with the others by assuming that the outer casing is insulated. The substrate slab from the right-hand end of the bioreactor is shown as the shaded slab dislocated to the right of the bioreactor. The bioreactor (as drawn) contains four of these substrate slabs (i.e., with $\times = 0$ on the right of the slab) and four mirror images (i.e., with $\times = 0$ on the left of the slab). Due to the symmetry, only one of these slabs needs to be modeled.

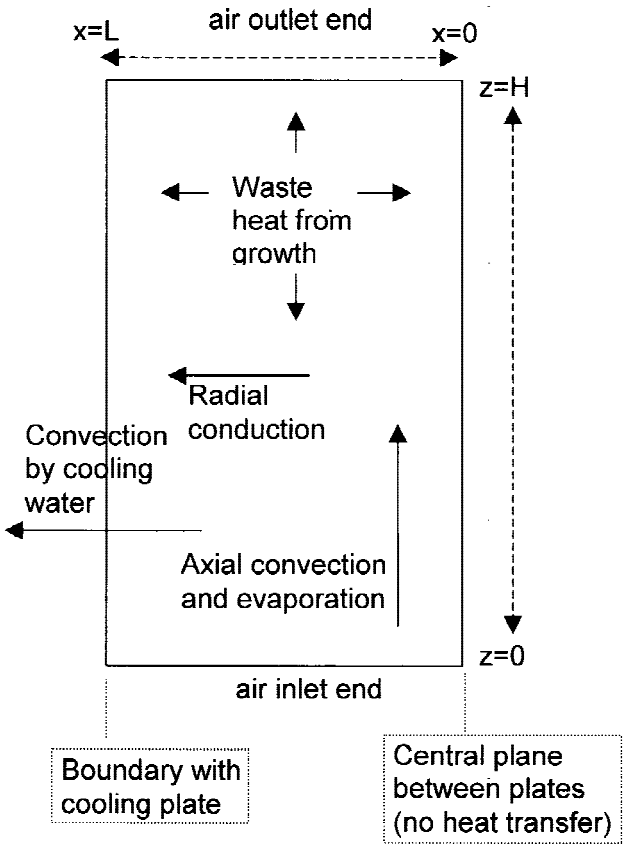


**Figure 2.** Diagram of the repeating unit of the Zymotis bioreactor, showing the geometry modeled. Since there are no front-to-back variations in the bioreactor, it can be represented by a rectangular plane given by a cross-section through the substrate slab, normal to the cooling plate.

### Growth Kinetics

The growth kinetics are described empirically by the logistic equation:

$$\frac{dX}{dt} = \mu X\left(1 - \frac{X}{X_m}\right) \tag{1}$$

The specific growth rate $\mu$ ($s^{-1}$) of *Aspergillus niger* is expressed empirically as a function of temperature (Saucedo-Castaneda et al., 1990):

$$\mu = \frac{A.\exp\left(\frac{-E_{a1}}{R(T + 273.16)}\right)}{1 + B.\exp\left(\frac{-E_{a2}}{R(T + 273.16)}\right)} \tag{2}$$

### Energy Balance

Figure 2 shows the heat transfer processes taken into account in the model. In the vertical direction it is assumed

that convection will dominate, and therefore vertical conduction is ignored. Since the air flows only in the vertical direction, there is no horizontal convection. Equation (3) is the macroscopic energy balance over the column:

$$\rho_b C_{pb}\left(\frac{\partial T}{\partial t}\right) + \rho_a(C_{pa} + f\lambda)V_z\left(\frac{\partial T}{\partial z}\right) = k_b\left(\frac{\partial^2 T}{\partial x^2}\right) + \rho_s(1-\varepsilon)Y\frac{dX}{dt} \quad (3)$$

The air and the moist solid at any particular location within the bed are assumed to be in thermal equilibrium, with the air saturated with water vapor. The factor $f\lambda$ arises since the evaporation of water to keep the air saturated gives the air a higher apparent heat capacity (Sangsurasak and Mitchell, 1998). Maintenance metabolism is ignored, as are effects of microbial growth on particle size and pressure drop across the bed.

Values for density, thermal conductivity, and heat capacity of the bed are calculated as weighted averages of the properties of the air and substrate within the bed. Density and thermal conductivity are volume-weighted, while heat capacity is mass-weighted:

$$\rho_b = \varepsilon.\rho_a + (1-\varepsilon)\rho_s \quad (4a)$$

$$k_b = \varepsilon.k_a + (1-\varepsilon)k_s \quad (4b)$$

$$C_{pb} = (\varepsilon\rho_a(C_{pa} + f.\lambda) + (1-\varepsilon)\rho_s C_{ps})/\rho_b \quad (4c)$$

Implicit in these equations is the assumption that the thermal properties of the microbe are equal to those of the substrate and that the void fraction does not change with time.

## Boundary and Initial Conditions

The bottom of the bed is maintained at the inlet air temperature, there is no heat transfer through the central plane between two cooling plates, and there is convective heat transfer from the edge of the bed to the cooling water:

$$z = 0 \qquad T = T_a \quad (5a)$$

$$x = 0 \qquad \frac{dT}{dx} = 0 \quad (5b)$$

$$x = L \qquad k_b\frac{dT}{dx} = -h(T - T_w) \quad (5c)$$

At the beginning of the fermentation, both the initial temperature ($T_o$) and the inoculum concentration ($X_o$) are assumed to be constant over the whole height (H) of the bed:

$$\text{at } t = 0 \qquad T = T_o \qquad 0 \le z \le H \quad (6a)$$

$$\text{at } t = 0 \qquad X = X_o \qquad 0 \le z \le H \quad (6a)$$

## Parameter Values

The parameters used in the model are given in Table I (Gumbira-Saíd et al., 1992; Himmelblau, 1982; Perry et al.,

**Table I.** Parameter values used in the model.

| Parameter | Value | Source |
|---|---|---|
| A | $7.483 \times 10^7$ s$^{-1}$ | Saucedo-Castaneda et al. (1990) |
| B | $1.300 \times 10^{47}$ | Saucedo-Castaneda et al. (1990) |
| $C_{pa}$ | 1180 J kg$^{-1}$ °C$^{-1}$ | Himmelblau (1982) |
| $C_{ps}$ | 2500 J kg$^{-1}$ °C$^{-1}$ | Sweat (1986) |
| $E_{a1}$ | 70225 J mol$^{-1}$ | Saucedo-Castaneda et al. (1990) |
| $E_{a2}$ | 283356 J mol$^{-1}$ | Saucedo-Castaneda et al. (1990) |
| f | 0.00246 kg-water kg-air$^{-1}$ °C$^{-1}$ | Himmelblau (1982) |
| h | 95 W m$^{-2}$ °C$^{-1}$ | Saucedo-Castaneda et al. (1990) |
| H | 0.035 m | Saucedo-Castaneda et al. (1990) |
| $k_a$ | 0.0206 W m$^{-1}$ °C$^{-1}$ | Perry et al. (1984) |
| $k_s$ | 0.3 W m$^{-1}$ °C$^{-1}$ | Van Lier et al. (1994) |
| L | 0.03 m | Saucedo-Castaneda et al. (1990) |
| R | 8.314 J mol$^{-1}$ °C$^{-1}$ | Himmelblau (1982) |
| $T_a$ | 35°C for Fig. 3, otherwise 25°C | Saucedo-Castaneda et al. (1990) |
| $T_o$ | 35°C for Fig. 3, otherwise 25°C | Saucedo-Castaneda et al. (1990) |
| $T_w$ | 35°C for Fig. 3, otherwise 25°C | Saucedo-Castaneda et al. (1990) |
| $T_{opt}$ | 38°C | Saucedo-Castaneda et al. (1990) |
| $V_z$ | 0.01 m s$^{-1}$ | Saucedo-Castaneda et al. (1990) |
| $X_o$ | 0.001 kg-biomass kg-substrate$^{-1}$ | Saucedo-Castaneda et al. (1990) |
| $X_m$ | 0.125 kg-biomass kg-substrate$^{-1}$ | Gumbira-Saíd et al. (1992) |
| Y | $8.366 \times 10^6$ J (kg biomass)$^{-1}$ | Saucedo-Castaneda et al. (1990) |
| $\varepsilon$ | 0.35 | Terzic and Todorovic (1992) |
| $\lambda$ | 2414300 J (kg water)$^{-1}$ | Himmelblau (1982) |
| $\rho_a$ | 1.14 kg m$^{-3}$ | Weast (1974) |
| $\rho_s$ | 700 kg m$^{-3}$ | Saucedo-Castaneda et al. (1990) |

Several of these parameters were varied for some of the simulations. In these cases the changes are noted in the text and figure legends.

1984; Saucedo-Castaneda et al., 1990; Sweat, 1986; Terzic and Todorovic, 1992, Van Lier et al., 1994; Weast, 1974). These parameters were estimated by Sangsurasak and Mitchell (1998) for the growth of *Aspergillus niger* on a starchy substrate in a packed-bed bioreactor, which was the system used by Saucedo-Castaneda et al. (1990).

Equation (4b) gives a value of $k_b$ of 0.20 W $m^{-1}$ $K^{-1}$, which is close to values measured experimentally by van Lier et al. (1994) of approximately 0.25 W $m^{-1}$ $K^{-1}$. Note that this value of $k_b$ represents the static bed conductivity. The repeated dividing and mixing of the air as it flows around particles in the bed leads to an extra mechanism parallel to radial conduction called eddy conduction (Froment and Bischoff, 1990). However, at the low particle Reynolds number of the order of 5 used in the simulations, the eddy conductivity was calculated to be an order of magnitude smaller than the static conductivity and was therefore ignored.

## Numerical Solution

The equation system was converted into dimensionless form, as shown in Table II. If the system were solved in this form, it would be numerically unstable due to the absence of the diffusion term in the vertical direction. In order to avoid instability problems, the method of characteristics is adopted, therefore the following modification is necessary:

$$\psi = \tau + 1/\alpha \cdot \zeta \tag{11a}$$

$$\omega = \zeta \tag{11b}$$

As a result, for any function G:

$$\left|\begin{array}{l} \dfrac{\partial G}{\partial \tau} = \dfrac{\partial G}{\partial \psi} \\ \dfrac{\partial G}{\partial \zeta} = \dfrac{1}{\alpha}\dfrac{\partial G}{\partial \psi} + \dfrac{\partial G}{\partial \omega} \end{array}\right. \tag{12}$$

The modified system was solved by applying polynomial approximation along variable $\varpi$, with $\alpha = 0$ and $\beta = 0.5$, and polynomial approximation along variable $\psi$, with $\alpha = 0$ and $\beta = 0$, in each case using the zeros of the Jacobi polynomials $(P^{(\alpha,\beta)})$ as interpolation points (Villadsen and Michelsen, 1978):

$$\theta(\chi, \omega, \psi) \cong \sum_{i=1}^{N+2} \ell_i(\chi) \cdot \theta_i(\omega, \psi) \tag{13}$$

$$\theta(\omega, \psi) \cong \sum_{j=1}^{N+1} \ell_j(\omega) \cdot \theta_{ij}(\psi) \tag{14}$$

where N is the number of internal collocation points. The resulting differential-algebraic system was solved using the DASSL routine (Petzold et al., 1989).

The numerical solution provides the temperature and the biomass at each collocation point. To allow comparison of different bioreactors, a volume-averaged biomass is calculated:

$$\overline{X}_{av} = \int_0^1 \int_0^1 \overline{X}(\chi, \omega, \psi)\, d\chi\, d\omega \cong \sum_{j=2}^{N+1} w_j \left( \sum_{i=2}^{N+1} w_i \cdot \overline{X}_{ij} \right) \tag{15}$$

where the *w*'s are weights of the Gauss' quadrature. This calculation is done for the cross-sectional area of the repeating unit within the bioreactor, but it represents a volume-average because there are no gradients from the front to the back of the bioreactor.

**Table II.** Dimensionless form of the model.

| Equation | No. |
|---|---|
| Dimensionless variables and constants | |
| $\tau = \dfrac{t.V_z}{H}$ | (7a) |
| $\zeta = \dfrac{z}{H}$ | (7b) |
| $\chi = \dfrac{x}{L}$ | (7c) |
| $\theta = \dfrac{T - T_o}{T_a}$ | (7d) |
| $\overline{X} = \dfrac{X - X_o}{X_m}$ | (7e) |
| $\alpha = \dfrac{-\rho_a(C_{pa} + f\lambda)}{\rho_b C_{pb}}$ | (7f) |
| $\beta = \dfrac{k_b H}{C_{pb}\rho_b V_z L^2}$ | (7g) |
| $\gamma = \dfrac{\rho_s Y(1-\varepsilon)X_m}{C_{pb}\rho_b T_a}$ | (7h) |
| $\eta = \dfrac{\mu H}{V_z}$ | (7i) |
| $\phi = \dfrac{hL}{k_b}$ | (7j) |
| Reformulated system of equations | |
| $\dfrac{\partial\theta}{\partial\tau} = \alpha\dfrac{\partial\theta}{\partial\zeta} + \beta\dfrac{\partial^2\theta}{\partial\chi^2} + \gamma\dfrac{\partial\overline{X}}{\partial\tau}$ | (8a) |
| $\dfrac{\partial\overline{X}}{\partial\tau} = \eta\left[\overline{X}\left(1 - \overline{X} - \dfrac{2X_o}{X_m}\right) + \dfrac{X_o}{X_m}\left(1 - \dfrac{X_o}{X_m}\right)\right]$ | (8b) |
| Initial conditions | |
| $\theta(0, \zeta, \chi) = 0$ | (9a) |
| $\overline{X}(0, \zeta, \chi) = 0$ | (9b) |
| Boundary conditions | |
| $\theta(\tau, 0, \chi) = 1 - \dfrac{T_o}{T_a}$ | (10a) |
| $\left.\dfrac{\partial\theta(\tau, \zeta, 0)}{\partial\chi}\right\|_{\chi=0} = 0$ | (10b) |
| $\left.\dfrac{\partial\theta(\tau, \zeta, 1)}{\partial\chi}\right\|_{\chi=1} = \phi\left(\theta + \dfrac{T_o}{T_a} - \dfrac{T_w}{T_a}\right)$ | (10c) |

## RESULTS

### Temperature and Biomass Gradients in a Zymotis Bioreactor

Figure 3 shows the predicted horizontal and vertical temperature gradients in a Zymotis bioreactor designed and operated using the parameters in Table I, which represent a system similar to that of Saucedo-Castaneda et al. (1990), who studied the growth of *Aspergillus niger* on whole cassava meal in a cylindrical packed-bed bioreactor of 35 cm height. The predictions are for 21.1 h, the time of peak heat production, as determined by inspection of the model output. Significant temperature profiles occur in both the vertical and horizontal directions, leading to corresponding biomass profiles. The highest temperatures occur toward the top and toward the center of the bioreactor and growth is poor in these regions. The biomass near the bottom and walls of the reactor has almost reached $X_m$, because the temperature has always been maintained close to $T_{opt}$, whereas the biomass near the top center is less than half $X_m$, indicating that the temperature there has been unfavorable for quite some time. The highest biomass concentration is at a position slightly above the bottom of the bioreactor because the inlet air temperature is lower than $T_{opt}$ and growth is better after the inlet air has been slightly warmed in the lowermost regions.

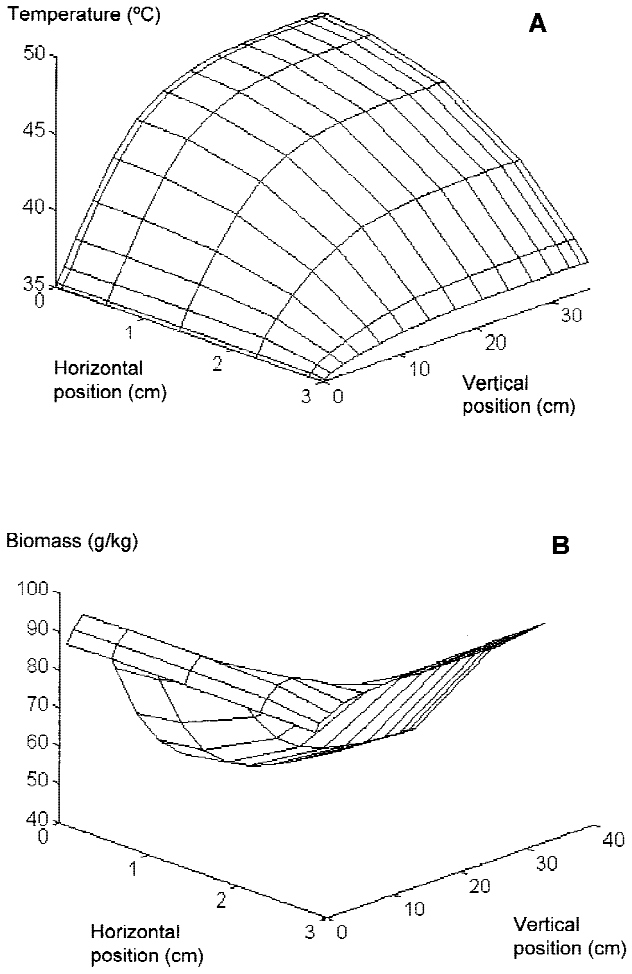


**Figure 3.** Model predictions demonstrating vertical and horizontal temperature (**A**) and biomass (**B**) gradients in a Zymotis bioreactor at the time of peak heat generation (21.1 h). The parameter values used are given in Table I, and give a system similar to that of Saucedo-Castaneda et al. (1990), but with a rectangular rather than cylindrical geometry.

The maximum temperature of 47°C predicted at the top of the substrate bed agrees well with the maximum temperature of 47.5°C obtained experimentally by Saucedo-Castaneda et al. (1990), who used a radius equal to the plate half-spacing (i.e., 3 cm). The predicted vertical temperature gradient is similar in shape to that observed by Saucedo-Castaneda et al. (1990): in the lower regions of the bed there is a significant vertical temperature gradient, followed by a transition, over a relatively short length of bed, to a region where the vertical temperature gradient is small. However, although the general trend is the same, the position of the transition point does not coincide. Experimentally, the transition point for the central axis of the cylindrical column is at a height of 5 cm (Saucedo-Castaneda et al., 1990). The transition in the model is smoother, and occurs at a height of around 10 cm.

The region near the top of the column in which there is only a slight axial temperature gradient represents the region where, due to the high temperature, the growth rate has decreased to a value for which the rate of metabolic heat release is approximately equal to the rate of heat removal by the cooling water. The rate of heat transfer to the cooling water is greater in this region than in the bottom of the column because the driving force is greater as a result of the higher bed temperature. The temperature gradient is more pronounced in the lower regions of the column because the temperature is closer to the optimum temperature for growth and therefore heat generation is higher. Heat transfer to the cooling water is not able to remove all this heat so some is removed by the air, meaning that the bed temperature increases with height. The position of the transition between the two regions changes with time during the fermentation because of the change in the rate of heat release by the biomass. The difference in the location of the transition points between the model and the experimental results arises because the cylindrical geometry of the bioreactor of Saucedo-Castaneda et al. (1990) leads to more effective heat transfer over the 3-cm column radius than occurs over the 3-cm plate half-spacing in the substrate slab described by the model. As a result, the balance between metabolic heat release and radial heat transfer occurs at a lower height and higher temperature. Saucedo-Castaneda et al. (1990) were not able to explain the shape of their experimental axial temperature profile because their model ignored axial heat transfer.

The aim of using a Zymotis bioreactor is to maximize the proportion of the energy removed by heat transfer to the cooling water, so that the vertical temperature gradient is minimized, relaxing the limitations on bioreactor height due to overheating considerations. Although the internal tem-

perature gradients are not plotted in the remaining simulations, the best performances correspond to conditions which maintain the column temperature, on average in both time and space, nearest to the optimal temperature for growth.

## Deriving a Criterion for Characterizing Bioreactor Performance

The spatial variations in biomass concentration (Fig. 3b) raise the question of how best to characterize the bioreactor performance. It is desirable to have a single number, for comparing the performance of bioreactors with different configurations and under different operating conditions. Sangsurasak and Mitchell (1995) characterized the performance of an ordinary packed-bed bioreactor on the basis of the growth at the hottest position in the bioreactor, namely, the center of the column at the outlet end of the bed, but this gives little information about the performance of the rest of the bed. The solution is to calculate a volume-averaged biomass concentration, as was done for tray bioreactors by Rajagopalan and Modak (1994), and to use this in a measure of productivity. Rajagoplan and Modak (1994) calculated the biomass concentration at 100 h, but such a simple measurement is insensitive to the shape of the growth curve. For example, it will not distinguish between two growth curves which give the same biomass concentration at 100 h: a curve which increases linearly between 0 and 100 h; and a curve which reaches the same final biomass concentration at 80 h and then enters a stationary phase. Therefore, bioreactor performance is characterized in the current work by noting the time for the volume-averaged biomass concentration to reach 90% of $X_m$. This time is denoted by the symbol "$t_{90}$". Note that a percentage of 90% of $X_m$ is arbitrary; other values could be used.

For comparison of the bioreactor performance against an absolute standard, the minimum possible value of $t_{90}$ can be calculated. If all of the bioreactor could be maintained at $T_{opt}$, then the growth curve would be described by the integrated logistic equation:

$$X = \frac{X_m}{1 + \left(\frac{X_m}{X_o} - 1\right)e^{-\mu t}} \tag{16}$$

with $\mu$ equal to its value for $T_{opt}$, which in the current work is 0.324 $h^{-1}$. Putting X at 90% of $X_m$ and solving for time gives 21.6 h as the minimum possible value of $t_{90}$.

## Sensitivity of Model Predictions to Heat Transfer Parameters

In wide ordinary packed-bed bioreactors, horizontal heat transfer is not important (Sangsurasak and Mitchell, 1995). However, it is crucial to the operation of Zymotis bioreactors, and therefore the parameters associated with horizontal heat transfer are also important. These parameters are the thermal conductivity of the substrate ($k_s$), which makes the major contribution to the thermal conductivity of the bed, and the heat transfer coefficient for convective cooling through the walls of the cooling plates (h). This section investigates the sensitivity of the model predictions to the values of these two parameters.

### *Sensitivity of the Model Predictions to $k_s$*

The thermal conductivity of a substrate varies significantly with its water content (Costa et al., 1998). Therefore, simulations were done with the parameters in Table I, with values of $k_s$ varying from 0.1 to 1.0 W $m^{-1}$ $K^{-1}$. This variation was done for two values of L (L = 0.05 and L = 0.2). It was done for a bed height of 2.5 m and a low superficial velocity of 0.01 m $s^{-1}$, conditions under which horizontal heat removal is crucial for good reactor performance.

With the plate half-spacing of L = 0.05 m, an increase in $k_s$ from 0.1 to 1.0 W $m^{-1}$ $K^{-1}$ reduces $t_{90}$ from 82 h to 45 h (Fig. 4). With the plate half-spacing of L = 0.2, although the 10-fold increase in $k_s$ reduces $t_{90}$ from 127 h to 101 h, this fermentation time is still quite prolonged, and the reduction in $t_{90}$ is relatively smaller than it was with the lower plate half-spacing. Therefore, regardless of the thermal conductivity of the substrate, the plate half-spacing must be small in order for adequate fermentation performance.

### *Sensitivity of the Model Predictions to the Value of h*

Again using the parameters in Table I, the value of h was varied from 50 to 250 W $m^{-2}$ $K^{-1}$, a typical range for the

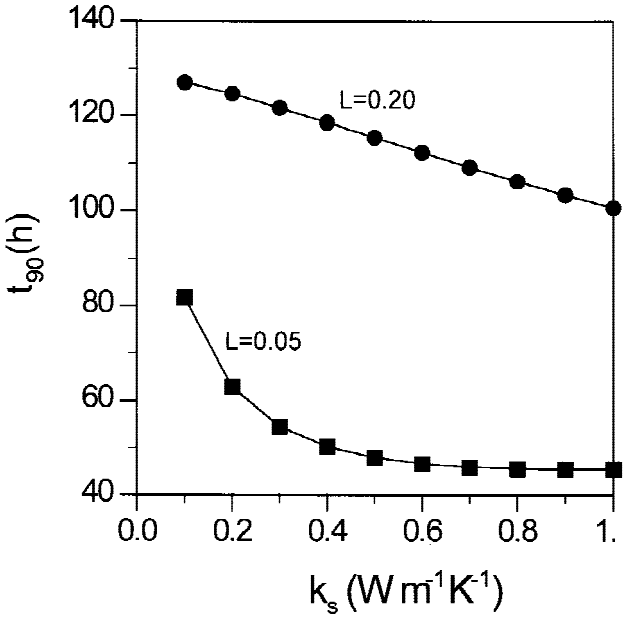


**Figure 4.** Sensitivity of the predicted time to reach 90% of $X_m$ ($t_{90}$) to the value of the thermal conductivity of the substrate ($k_s$). (■) Predictions for a plate half-spacing of 0.05 m; (●) Predictions for a plate half-spacing of 0.2 m. The reactor height is 2.5 m. The other model parameters are as given in Table I.

overall heat transfer coefficient for plate heat exchangers (Perry et al., 1984). The bed height was 2.5 m, the superficial velocity 0.01 m $s^{-1}$, and the half-plate spacing 0.05 m. With the 5-fold increase in h, $t_{90}$ decreases only from 55.9 h to 53.7 h, indicating that the major resistance to horizontal heat transfer is within the substrate bed itself. This confirms the importance of the plate half-spacing as a design decision.

## Operability

The aim of the current work is explore how Zymotis bioreactors should be designed and operated. For ordinary packed beds, superficial velocity, the temperature of the inlet air, and the height of the bioreactor have the most effect on bioreactor performance (Sangsurasak and Mitchell, 1995). The current work concentrates on the interrelationships between these parameters and two parameters associated with the internal cooling plates, namely, the half-plate spacing (L) and the temperature of the cooling water. The parameters are as given in Table I, with various operating parameters being varied from this base case.

### *Effect of Design Variables on Bioreactor Performance*

Figure 5 shows the predicted values of $t_{90}$ for various bioreactor heights (H) and plate half-spacings (L), for a superficial velocity of 0.01 m $s^{-1}$. Regardless of the plate half-spacing, $t_{90}$ increases approximately linearly with H, because more of the bioreactor is at temperatures away from $T_{opt}$ during the fermentation. In contrast, the reliance of $t_{90}$ on L at constant H is not linear. As L increases from 0.05 to 0.15 m, $t_{90}$ increases sharply, with the sharpness of this increase increasing with H. However, as L increases further above 0.15 there is little change in $t_{90}$, indicating that horizontal heat transfer is contributing a negligible proportion of the overall heat removal at these plate half-spacings. Therefore, in the following simulations results are not shown for values of L above 0.15 m.

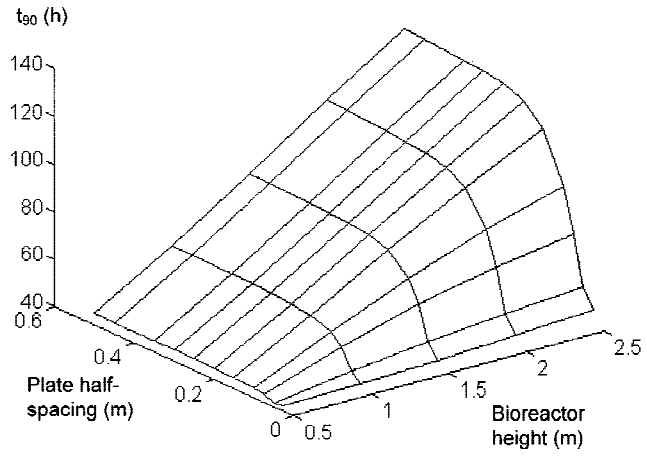


**Figure 5.** Effect of the bioreactor configuration on the time required to reach 90% of $X_m$ ($t_{90}$). The other model parameters are as given in Table I.

Figure 5 suggests that reasonable performances can be obtained with a bioreactor height of 2.5 m, although the lowest value for $t_{90}$ (41.7 h) is still far from the minimum possible value of 21.6 h. This bioreactor height was used for the remaining simulations, in order to explore the potential of the Zymotis bioreactor for large-scale operation.

### *Effect of Operating Variables on Bioreactor Performance*

The model was used to search for those operating variables with the most potential to improve bioreactor performance. In each case the variations were made from the base case given in Table I. The effect of each operating variable was investigated over a range of plate half-spacings from 0.025 to 0.15 m. Details of the simulation results are not shown, but the main points are summarized below.

Superficial velocity was varied from 0.01 m $s^{-1}$, which has been used quite commonly in packed beds, to 0.03 $ms^{-1}$, which is slightly higher than the highest value of 0.024 m $s^{-1}$ used by Ghildyal et al. (1994). Performance was best with high values of $V_z$ and low values of L. However, the lowest value of $t_{90}$, obtained at $V_Z = 0.03$ m $s^{-1}$ and L = 0.025 m, was 42.3 h, which is far from the minimum possible value of 21.6 h.

The cooling water temperature was varied from 10°C to 40°C. The lowest value of $t_{90}$ was 38.0 h with a plate half-spacing of 0.025 m and a cooling water temperature of 30°C. This relatively high optimum cooling water temperature occurs because lower cooling water temperatures initially cool the bed significantly below the optimal temperature for growth, retarding the initial growth significantly.

The process air temperature was varied from 10°C to 45°C. The minimum value of $t_{90}$ of 44.9 h was obtained with a plate half-spacing of 0.025 m, and a process air temperature of 40°C. Optimal performance at a temperature slightly higher than the $T_{opt}$ of 38°C occurs because this air temperature counterbalances the overcooling early during the fermentation caused by the cooling water temperature of 25°C. During the period of peak heat removal this high air temperature is unimportant because the majority of the heat is removed by the cooling water.

Summarizing the effects of the operating variables, the best performance was obtained at the lowest value of the plate half-spacing tested, and by optimizing the temperature of the cooling water. However, if the temperature of the cooling water is maintained constant during the process, then it is difficult to reduce $t_{90}$ toward the minimum possible value of 21.6 h, because a cooling water temperature that cools effectively during the period of peak heat removal overcools the bed early in the process when the heat generation rate is very low. This leads to the idea of keeping $T_w$ near $T_{opt}$ at the beginning of the fermentation and then decreasing it during the period of rapid growth. It was therefore assumed that a thermocouple inserted at (x,z) = (L,H)

measures the temperature at this point ($T_{LH}$) and controls $T_w$ as follows:

$$T_w = T_{opt} - F^*(T_{LH} - T_{opt}) \quad (17)$$

where F controls the degree with which $T_w$ decreases as $T_{LH}$ increases. To keep the column temperature as close as possible to $T_{opt}$ during early growth, $T_a$ was set at $T_{opt}$.

Figure 6 shows the effect of F on $t_{90}$, at $V_z = 0.03$ m $s^{-1}$, for values for the plate half-spacing of 0.025 and 0.05 m. The hope was that L = 0.05 m would work well, as this larger plate half-spacing would facilitate loading and unloading of the bioreactor. However, the best $t_{90}$ value was above 30 h. With L = 0.025 m the optimal performance ($t_{90}$ = 21.6 h) was approached, with $t_{90}$ ranging from 29.4 h for F = 1 down to 26.5 h for F = 5. The minimum $T_w$ values ranged from 31.5 to 23.5°C. Such cooling water temperatures are available in most parts of the world, without the need for refrigeration.

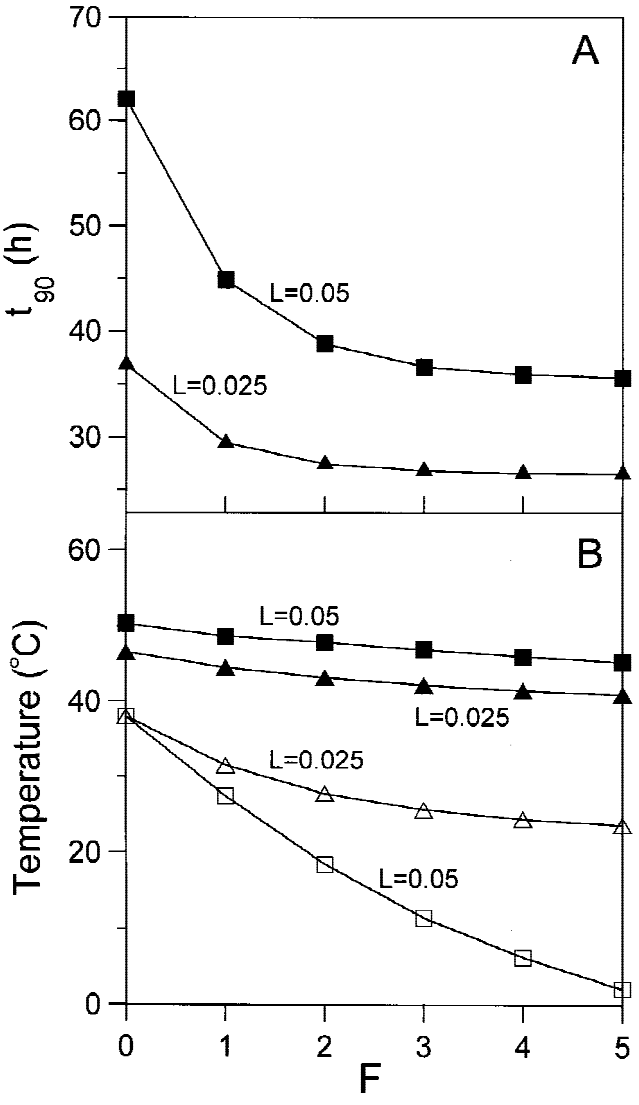


**Figure 6.** Effect of controlling the cooling water temperature during the fermentation, plotted against the factor F used in the control algorithm given by Eq. (17). The bioreactor is 2.5 m tall and the superficial velocity is 0.03 m $s^{-1}$. The other parameter values are as given in Table I. The results are plotted for two plate half-spacings: triangles represent L = 0.025 m and squares represent L = 0.05 m. (**A**) Time to reach 90% $X_m$; (**B**) Maximum temperature reached in the column (solid symbols) and the minimum temperature of the cooling water (hollow symbols).

The idea of profiling fermentation temperatures to optimize growth in SSF processes was suggested by Sargantanis et al. (1993) but they simply calculated, as a function of time, the temperature at which the bed should be held in order to maximize the growth rate. They did not show how the bioreactor should be operated to keep the substrate bed at the desired temperature. The current control algorithm shows how the operating variables should be changed as a function of time.

## Evaluating the Potential of the Zymotis Bioreactor

The Zymotis bioreactor was proposed in 1993 by Roussos et al., but has received little attention. The current work enables evaluation of its potential. In summary, the Zymotis bioreactor can perform reasonably close to the optimal possible performance, as evidenced by a $t_{90}$ of 26.5 h (Fig. 6), compared to the minimum possible $t_{90}$ of 21.6 h. The disadvantage is that, to achieve this good performance with a fast-growing organism such as *Aspergillus niger*, the plate half-spacing must be 0.025 m, meaning that the gap between plates is only 5 cm. Such small gaps complicate the operations of loading and unloading of the bioreactor. As a result, the Zymotis bioreactor has an ease of use and handling similar to that of trays.

For SSF processes in which the substrate bed cannot be stirred during the fermentation, the only options available are the tray, the ordinary packed-bed, and the Zymotis bioreactor. The limitations of the ordinary packed-bed at widths which would be required for large-scale operation are already clear (Sangsurasak and Mitchell, 1995, 1998), and are apparent in the current work by looking at the results for large values of L. The limitations of trays were shown by Rajagopalan and Modak (1994), who also based their growth kinetics on the work of Saucedo-Castaneda et al. (1990): For a substrate bed thickness of 6.35 cm, and varying the temperature of the surrounding air from 25–45°C, the best performance obtained was a biomass concentration of 55% of $X_m$ after 100 h of fermentation. Growth was significantly limited by the poor heat removal. The heat removal in the Zymotis bioreactor is much better than in trays, first because of the convective air flow through the bed, and second because, at the edge of the bed, the convective heat removal by the cooling water is more effective than the convective heat removal by the headspace air within the tray chamber. Furthermore, $O_2$ depletion can be a problem in trays (Rajagopalan and Modak, 1994), but it is avoided in the Zymotis bioreactor due to the forced aeration. Therefore, of the three bioreactor types available for static SSF processes, the Zymotis bioreactor has the best potential.

## CONCLUSIONS

We used mathematical modeling as a tool to evaluate the potential of the Zymotis bioreactor, and to identify those design and operating variables with the greatest effect on bioreactor performance. Regarding the potential of the Zymotis bioreactor, we have shown that it has potential to minimize the degree to which growth is restricted by heat transfer limitations, leading to a bioreactor performance reasonably close to the best possible performance. Regarding the design and operating variables, $V_z$, L, and $T_w$ are of major importance. $V_z$ is important in ordinary wide packed-bed bioreactors, but the importance of the other two parameters results from the presence of the internal heat transfer plates in the Zymotis design. The best strategy is to use a small L, a high $V_z$, and to vary the value of $T_w$ during the fermentation in response to the bed temperature. The interactions between L, $T_w$, $T_a$, and $V_z$ are quite complex, which highlights the importance of using mathematical modeling as a tool in optimizing the design and operation of SSF bioreactors.

## NOMENCLATURE

- A Frequency factor ($s^{-1}$)
- B Constant in Arrhenius equation (dimensionless)
- $C_{pa}$ Heat capacity of the air phase (J $kg^{-1}$ °$C^{-1}$)
- $C_{pb}$ Heat capacity of the bed (J $kg^{-1}$ °$C^{-1}$)
- $C_{ps}$ Heat capacity of the substrate (J $kg^{-1}$ °$C^{-1}$)
- $E_{a1}$ Activation energy (J $mol^{-1}$ °$C^{-1}$)
- $E_{a2}$ Inactivation energy (J $mol^{-1}$ °$C^{-1}$)
- f Change in water carrying capacity of air with temperature (kg-water kg-$air^{-1}$ °$C^{-1}$)
- F Factor used in the scheme for controlling cooling water temperature (dimensionless)
- h Coefficient for convective cooling across the bioreactor wall from × = L to the cooling water (W $m^{-2}$ °$C^{-1}$)
- H Overall height of the bed (m)
- $k_a$ Thermal conductivity of the air phase (W $m^{-1}$ °$C^{-1}$)
- $k_b$ Thermal conductivity of the bed (W $m^{-1}$ °$C^{-1}$)
- $k_s$ Thermal conductivity of the substrate phase (W $m^{-1}$ °$C^{-1}$)
- L Half of the distance between two heat-transfer plates ("plate half-spacing", m)
- R Universal gas constant (J $mol^{-1}$ °$C^{-1}$)
- t Time (s)
- $t_{90}$ Time for the volume-averaged biomass concentration to reach 90% of $X_m$ (h)
- T Temperature (°C)
- $T_a$ Inlet air temperature (°C)
- $T_{LH}$ Temperature at × = L and z = H (°C)
- $T_o$ Initial bed temperature (°C)
- $T_{opt}$ Optimum temperature for growth (°C)
- $T_w$ Cooling water temperature (°C)
- $V_z$ Superficial air velocity (m $s^{-1}$)
- x Horizontal position within bed (m)
- X Biomass concentration (kg-biomass kg-$substrate^{-1}$)
- $X_m$ Maximum biomass concentration (kg-biomass kg-$substrate^{-1}$)
- $X_o$ Initial biomass concentration (kg-biomass kg-$substrate^{-1}$)
- Y Heat yield coefficient (J kg-$biomass^{-1}$)
- z Vertical position within bed (m)
- $\varepsilon$ Void fraction (dimensionless)
- $\lambda$ Enthalpy of vaporization of water (J $kg^{-1}$)
- $\rho_a$ Density of air (kg $m^{-3}$)
- $\rho_b$ Density of the bed (kg $m^{-3}$)
- $\rho_s$ Density of substrate (kg $m^{-3}$)
- $\mu$ Specific growth rate ($s^{-1}$)

## References


Boyette CD, Quimby PC Jr, Connick WJ Jr, Daigle DJ, Fulgham FE. 1991. Progress in the production, formulation and application of mycoherbicides. In: TeBeest DO, editor. Microbial control of weeds. New York: Chapman & Hall. p 209–222.

Costa JAV, Alegre RM, Hasan SDM. 1998. Packing density and thermal conductivity determination for rice bran solid-state fermentation. Biotechnol Tech 12:747–750.

Froment OF, Bischoff KB. 1990. Chemical reactor analysis and design, 2nd ed. New York: Wiley.

Ghildyal NP, Gowthaman MK, Raghava Rao KSMS, Karanth NG. 1994. Interaction between transport resistances with biochemical reaction in packed bed solid-state fermentors: effect of temperature gradients. Enzyme Microb Technol 16:253–257.

Gumbira-Saíd E, Mitchell DA, Greenfield PF, Doelle HW. 1992. A packed bed solid-state fermentation system for the production of animal feed: cultivation, drying and product quality. Biotechnol Lett 14:623–628.

Himmelblau DM. 1982. Basic principles and calculations in chemical engineering, 5th ed. Englewood Cliffs, NJ: Prentice Hall.

Morin L. 1992. Realizing the potential of bioherbicides. Plant Prod Q 7:143–148.

Perry RH, Green DW, Maloney JO. 1984. Perry's chemical engineer's handbook, 5th ed. New York: McGraw-Hill.

Petzold LR, Brenan KE, Campbell SL. 1989. Numerical solution of initial-value problems in differential-algebraic equations. New York: Elsevier.

Rajagopalan S, Modak JM. 1994. Heat and mass transfer simulation studies for solid-state fermentation processes. Chem Eng Sci 49:2187–2193.

Roussos S, Raimbault M, Prebois J-P, Lonsane BK. 1993. Zymotis, a large scale solid state fermenter. Appl Biochem Biotechnol 42:37–52.

Sangsurasak P, Mitchell DA. 1995. Incorporation of death kinetics into a 2-D dynamic heat transfer model for solid state fermentation. J Chem Technol Biotechnol 64:253–260.

Sangsurasak P, Mitchell DA. 1998. Validation of a model describing 2-dimensional heat transfer during solid-state fermentation in packed bed bioreactors. Biotechnol Bioeng 60:739–749.

Sargantanis J, Karim MN, Murphy VG, Ryoo D, Tengerdy RP. 1993. Effect of operating conditions on solid substrate fermentation. Biotechnol Bioeng 42:149–158.

Saucedo-Castaneda G, Gutierrez-Rojas M, Bacquet G, Raimbault M, Viniegra-Gonzalez G. 1990. Heat transfer simulation in solid substrate fermentation. Biotechnol Bioeng 35:802–808.

Silman RW. 1980. Enzyme formation during solid-substrate fermentation in rotating vessels. Biotechnol Bioeng 22:411–420.

Sweat VE. 1986. Thermal properties of foods. In: Rao MA, Rizvi SS, editors. Engineering properties of foods. New York: Marcel Dekker. p 49–132.

Terzic MS, Todorovic MS. 1992. The experimental investigation of isothermal and nonisothermal fluid flow and heat transfer through porous media. In: Quintard M, Todorovic M, editors. Heat and mass transfer in porous media. Amsterdam: Elsevier. p 585–600.

Van Lier JJC, Van Ginkel JT, Straatsma G, Gerrits JPG, Van Griensven LJLD. 1994. Composting of mushroom substrate in a fermentation tunnel: compost parameters and a mathematical model. Netherlands J Agr Sci 42:271–292.

Villadsen J, Michelsen ML. 1978. Solution of differential equation models by polynomials approximation. Englewood Cliffs, NJ: Prentice-Hall.

Weast RC. 1974. Handbook of chemistry and physics, 55th ed. Cincinnati: CRC Press.